Journal of Natural Gas Science and Engineering 39 (2017) 72–81

Contents lists available at ScienceDirect

Journal of Natural Gas Science and Engineering

journal homepage: www.elsevier.com/locate/jngse

Fluid factor index for fluid saturation estimation

Xuehui Han [a], Enfan Wu [a], Junxin Guo [a,*], Denghui Xu [a], Zhongchun Sun [b], Xingping Luo [b], Zhenlin Wang [b], Long Yang [c]

[a] School of Geoscience, China University of Petroleum (East China), Qingdao 266580, China
[b] Research Institute of Exploration and Development of PetroChina Xinjiang Oilfield Company, China
[c] Research Institute of Experiment and Detection of PetroChina Xinjiang Oilfield Company, China

ARTICLE INFO

Article history:
Received 22 August 2016
Received in revised form
26 January 2017
Accepted 28 January 2017
Available online 3 February 2017

Keywords:
Fluid factor index
Fluid saturation
Porosity
Sensitivity
Sandstone

ABSTRACT

Estimation of fluid saturation is of great importance to the oil/gas exploration and production. In this work, we propose the fluid factor index for the fluid saturation estimation. The fluid factor index is defined as the ratio of the value of the fluid factor for rocks with oil/gas-water saturation to the corresponding value under the full water saturation. Similar with the resistivity index in Archie's formula, this definition of fluid factor index can largely cancel out the influences of rock porosities and hence primarily reflects the effects of fluid saturation. Five fluid factor indices (I_K, $I_{\Delta K}$, $I_{VP/VS}$, I_ν, and I_{Zp}) are then studied, which are calculated from sample bulk modulus, bulk modulus increment due to fluid saturation, compressional to shear velocity ratio, Poisson's ratio, and compressional wave impedance, respectively. Their sensitivities to the fluid saturation and their dependency on rock porosities are investigated through the ultrasonic experiments on the water-oil and water-gas saturated sandstone samples. The results show that, for both the water-oil and water-gas saturated samples, $I_{\Delta K}$ is an ideal fluid factor index for fluid saturation estimation as it is most sensitive to the fluid saturation and is almost independent of the rock porosities; I_K and I_ν are not as good as $I_{\Delta K}$, but are better than $I_{VP/VS}$ and I_{Zp} with respect to their sensitivity to the fluid saturation and dependency on the rock porosities. Hence, $I_{\Delta K}$ is recommended to be used for the fluid saturation estimation. These experimental observations can be validated and explained by the theoretical simulations. This research provides the basis for using the acoustic data to estimate the fluid saturation, which is very helpful to the oil/gas exploration and production.

1. Introduction

Reservoir fluid saturation estimation is of great importance to the oil/gas exploration and production. The fluid saturation is often correlated to the geophysical parameters by theoretical models or experimental empirical formulas, which enables the estimation of the fluid saturation from the measured geophysical parameters. To this end, the resistivity or conductivity of the formation rocks are most often measured by well logging and used for fluid saturation estimation.

Up until now, a number of models have been proposed to correlate the formation electrical properties with the fluid saturation. Among them, the most widely used model is the Archie's formula (Archie, 1942), which is based on the measurement of the electrical properties of the clean sandstone with varying water saturation. While this formula was proposed for the clean sandstone, it has been used extensively for many other reservoir rocks, such as the shaly sandstone, through modifying the coefficients in the formula (Salem and Chilingarian, 1999; Ara et al., 2001; Rezaee et al., 2007; Olsen et al., 2008; Teh et al., 2011; Hamada et al., 2013). Besides the Archie's formula, there are also many other models developed for the specific reservoir types, such as the Waxman-Smits model (Waxman and Smits, 1968) and the Dual-Water model (Clavier et al., 1984) for the shaly sandstone, and the Triple-Porosity model for carbonate rocks (Gao et al., 2015).

Apart from estimating the fluid saturation from the electrical properties of the formation rocks, the methods using the elastic properties of the formation rocks are also developed in recent years. To enable the estimation of fluid saturation from the rock elastic properties, we need to obtain the elastic parameters that are sensitive to the fluid saturation and build their quantitative relations with the fluid saturation. These sensitive elastic parameters are often called the fluid factors. Up to date, various types of fluid

* Corresponding author.
E-mail address: guojunxin1989@gmail.com (J. Guo).

http://dx.doi.org/10.1016/j.jngse.2017.01.026
1875-5100/

factors have been proposed. For instance, Hilterman (1989) applied the reflectivity of Poisson's ratio to denote the anomalies of the oil and gas, which showed good results. Batzle et al. (2001) carried out the experiments and obtained a fluid factor which is expressed as the difference between the bulk and shear moduli. Russell et al. (2003) pointed out that the fluid term in the Gassmann equation has good relation with the fluid properties. Hence, they obtain a fluid factor as the product of the fluid term in Gassmann equation with the density. Ning et al. (2006) analyzed the numerous fluid factors, based on which the general form of the fluid factors is given. It is formed by the compressional and shear wave impedance, and their combinations.

When estimating the fluid saturation from the fluid factors, the fluid saturation is often correlated to the absolute values of the fluid factors. However, the absolute values of the fluid factors can be greatly influenced by the rock porosities (Yin et al., 2015). Hence, the fluid saturation estimation accuracy will be largely affected by the accuracy of the rock porosity data. To reduce the influences of the rock porosities on the fluid saturation estimation results, we propose the fluid factor index in this paper in a similar way with the resistivity index in the Archie's formula, that is, the ratio of the value of the fluid factor for rocks with oil/gas-water saturation to the corresponding value under the full water saturation. As the fluid factors are divided by the corresponding values for rocks saturated with water, the influences of the rock porosities can be largely cancelled out and hence the fluid factor indices will primarily reflect the influences of the fluid saturation, just as the resistivity index. Using the fluid factor indices will thus enable the more accurate estimation of fluid saturations.

In this paper, we will propose several fluid factor indices. Their sensitivities to the fluid saturation and also their dependencies on rock porosities will be investigated through the ultrasonic experiments on the oil-water and gas-water saturated sandstone samples. Furthermore, the theoretical simulations will also be carried out to validate and explain the experimental results.

2. Experiments

2.1. Ultrasonic measurements on sandstone samples

Two sets of sandstone samples are used in this study. One set of samples are from Daqing Oilfield of China and the other set of samples are from Xinjiang Oilfield of China. The distributions of the porosities of these two sets of samples are shown in Tables 1 and 2, respectively. The samples from Daqing Oilfield are saturated with water-oil mixture and those from Xinjiang Oilfield are saturated with water-gas mixture. As the porosities and permeability of both sets of samples are not small, the fluid saturation can be changed through displacing oil by water for samples of Daqing Oilfield and displacing water by gas for samples of Xinjiang Oilfield. Hence, we can measure the ultrasonic velocities of the samples at different fluid saturations. The fluid factor indices can then be calculated, and analyzed with respect to their sensitivities to the fluid saturation and dependencies on the rock porosities.

The ultrasonic velocities of the saturated samples are measured using a multiple acoustic parameter measurement system. The central frequencies of the transducers for the compressional and shear waves are 0.25 MHz and 0.12 MHz, respectively. The acoustic velocities are measured using the ultrasonic transmission method. The acoustic wave transmission time through the sample is measured, which enables the calculation of the acoustic wave velocity as follows:

$$V = \frac{L}{t}, \tag{1}$$

where V is the acoustic wave velocity; L is the length of the sample; t is the acoustic wave transmission time through the sample.

The relative measurement uncertainties for the compressional and shear wave velocities are smaller than 0.5% and 1%, respectively. The measurements are carried out under the in-situ confining pressure (23 MPa) and temperature (40 °C) of the formations. To ensure the accuracy of the measurements, each velocity is measured at least three times.

Table 1
The porosity distribution of the water-oil saturated sandstone samples from Daqing Oilfield, China.

Sample No.	Porosity	Sample No.	Porosity
D 46	0.1017	D 52	0.1245
D 48	0.1261	D 32	0.1323
D 23	0.1575	D 38	0.1755

Table 2
The porosity distribution of the water-gas saturated sandstone samples from Xinjiang Oilfield, China.

Sample No.	Porosity
2212	0.1389
2221	0.1983
2213	0.2003

2.2. Selection of fluid factor indices

The sandstone samples in this study have the property of isotropy. Hence, once the compressional and shear wave velocities of the samples are measured, the bulk and shear moduli of the samples can be obtained as follows:

$$K = \rho\left(V_p^2 - \frac{4}{3}V_s^2\right), \tag{2}$$

$$G = \rho V_s^2, \tag{3}$$

where K and G are the bulk and shear moduli of the samples, respectively; V_p and V_s are the measured compressional and shear wave velocities, respectively; ρ is the sample density, which can be calculated through the weight and volume of the samples.

Using the bulk and shear moduli of these samples, various fluid factor indices can be computed. Since the fluid has significant influences on the bulk moduli of the samples and negligible effects on the sample shear moduli (Gassmann, 1951), we select the bulk modulus related fluid factor indices for investigation. Hence, the most direct fluid factor index is the ratio of the bulk modulus to that of the sample saturated with water:

$$I_K = K/K_0, \tag{4}$$

where K_0 is the bulk modulus of the sample saturated with water.

The bulk modulus increment due to fluid saturation ΔK is proved to be a good fluid factor by Han and Batzle (2004). Hence, we can obtain another fluid factor index $I_{\Delta K}$ as follows:

$$\Delta K = K - K_d, \tag{5}$$

$$\Delta K_0 = K_0 - K_d, \tag{6}$$

$$I_{\Delta K} = \Delta K / \Delta K_0, \tag{7}$$

where K_d is the bulk modulus of the dry samples, which can be calculated from the acoustic velocities and density of the dry samples using equation (2).

Besides these two fluid factor indices $I_{\Delta K}$ and I_K, we also obtain the fluid factor indices from the ratio of compressional wave velocity to shear wave velocity V_p/V_s, the Poisson's ratio ν, and the compressional wave impedance Z_p, which are related to the bulk modulus as follows:

$$\frac{V_p}{V_s} = \sqrt{\frac{K + 4/3G}{G}}, \tag{8}$$

$$\nu = \frac{3K - 2G}{2(3K + G)}, \tag{9}$$

$$Z_p = \sqrt{(K + 4/3G)\rho}. \tag{10}$$

The corresponding fluid factor indices are as follows:

$$I_{V_p/V_s} = \frac{V_p/V_s}{V_{p0}/V_{s0}}, \tag{11}$$

$$I_\nu = \frac{\nu}{\nu_0}, \tag{12}$$

$$I_{Z_p} = \frac{Z_p}{Z_{p0}}, \tag{13}$$

where the index 0 denotes the values for the sample saturated with water.

In the following, we will analyze the variations of these fluid factor indices with the fluid (water) saturation and their dependencies on the rock porosities.

3. Results

3.1. Samples saturated with water-oil mixture from Daqing Oilfield

Fig. 1(a) shows the variation of the fluid factor index I_K with the water saturation for the water-oil saturated samples under different porosities. It can be seen that I_K increases with the water saturation. This is because the effective fluid modulus increases with the water saturation, which results in the increase of the bulk modulus of the saturated samples. It can also be found that the influences of the porosities on the variations of I_K with water saturation are not totally cancelled out. I_K for the samples with larger porosities are found to be more sensitive to the water saturation variation. For the sample with the smallest porosity (D46), the change of I_K from $S_w = 0$ to $S_w = 1$ is 0.15, whereas that for the sample with the largest porosity (D38) is 0.225. Hence, the relative change of I_K due to the influences of the porosity [(0.225−0.15)/0.225] is around 33%, which is not negligible. The variation of I_K with the porosity indicates that the rock porosity has different effects on the bulk modulus of the samples saturated with water and those saturated with water-oil mixture. As a result, the effects of porosity are not cancelled out and hence I_K depends on porosity.

The variations of $I_{\Delta K}$ with the water saturation is given in Fig. 1(b). It can be found that this fluid factor index also increases with the water saturation. As the bulk modulus of the saturated sample increases with the water saturation, its relative increment relative to the bulk modulus of the dry sample ΔK also increases. Hence, $I_{\Delta K}$ will increase with the water saturation. Compared with I_K, it can be clearly seen that $I_{\Delta K}$ is much more sensitive to the water saturation. It can also be found that the porosity also has some effects on the variation of $I_{\Delta K}$ with the water saturation. The larger the porosity, the more sensitive the fluid factor index $I_{\Delta K}$ to the water saturation variation. However, its relative change with the porosity is much smaller than that of I_K. For instance, the change of $I_{\Delta K}$ from $S_w = 0$ to $S_w = 1$for the sample with the smallest porosity (D46) is 0.4, whereas that for the sample with the largest porosity (D38) is 0.5. Therefore, the relative change of $I_{\Delta K}$ due to the effects of the porosity [(0.5−0.4)/0.5] is around 20%, which is much smaller than that of I_K. The small dependence of $I_{\Delta K}$ on the porosity means the influences of porosity on the samples saturated with water-oil mixture and those saturated with water can be largely cancelled out. This can be explained by theory, which will be discussed in the next section.

The variation of the fluid factor index $I_{VP/VS}$ with the water saturation is shown in Fig. 1(c). Due to the increase of the bulk modulus of the saturated samples with the water saturation, the compressional wave velocity increases with the water saturation while the shear wave velocity keeps constant. Hence, this fluid factor index increases with the water saturation. It can be observed that its sensitivity to the water saturation is smaller than that of I_K and $I_{\Delta K}$. However, its dependency on the porosity is much larger than I_K and $I_{\Delta K}$. The relative change of $I_{VP/VS}$ between the sample with the smallest and largest porosity is around 50%. Hence, this fluid factor is not as good as I_K and $I_{\Delta K}$.

Fig. 1(d) shows the variations of I_ν with the water saturation. Since the bulk modulus of the saturated samples increases with the water saturation and the shear modulus keeps constant, this fluid factor also increases with the water saturation according to equations (9) and (12). It can be seen that the sensitivity of this fluid factor index to the water saturation is slightly lower than that of I_K. However, it has less dependency on porosity than I_K. The relative change of I_ν between the sample with the smallest and largest porosity is around 25%, which is close to that of $I_{\Delta K}$. Hence, considering both the sensitivity to the water saturation and the dependency on the porosity of this fluid factor index, it is also a good fluid factor index for the fluid saturation estimation.

The variation of I_{Zp} with the water saturation is shown in Fig. 1(e). It can be seen that the sensitivity of this fluid factor index to water saturation is lowest among these five fluid factor indices. Its dependency on the porosity can also be denoted using the relative change of this fluid factor index between the sample with the largest porosity and that with the smallest porosity, whose value is around 46%. This value is nearly as large as that of $I_{VP/VS}$. Hence, this fluid factor index is not good as it is not sensitive to the water saturation and are largely dependent on the porosity compared with the other fluid factor indices.

In summary, with respect to the sensitivities of these fluid factor indices to the water saturation for the water-oil saturated sandstone, we can obtain the relation: $I_{\Delta K} > I_K > I_\nu > I_{VP/VS} > I_{Zp}$. For the dependency of these fluid factor indices on the rock porosity, we have $I_{\Delta K} < I_\nu < I_K < I_{Zp} < I_{VP/VS}$. A good fluid factor index should have high sensitivity to the water saturation and low dependency on the porosity. Hence, for the fluid saturation estimation in water-oil saturated sandstone, the best fluid factor index is $I_{\Delta K}$, I_K and I_ν are secondary, and $I_{VP/VS}$ and I_{Zp} are worst.

3.2. Samples saturated with water-gas mixture from Xinjiang Oilfield

The variations of the various fluid factor indices with the water saturation for the samples saturated with water-gas mixture

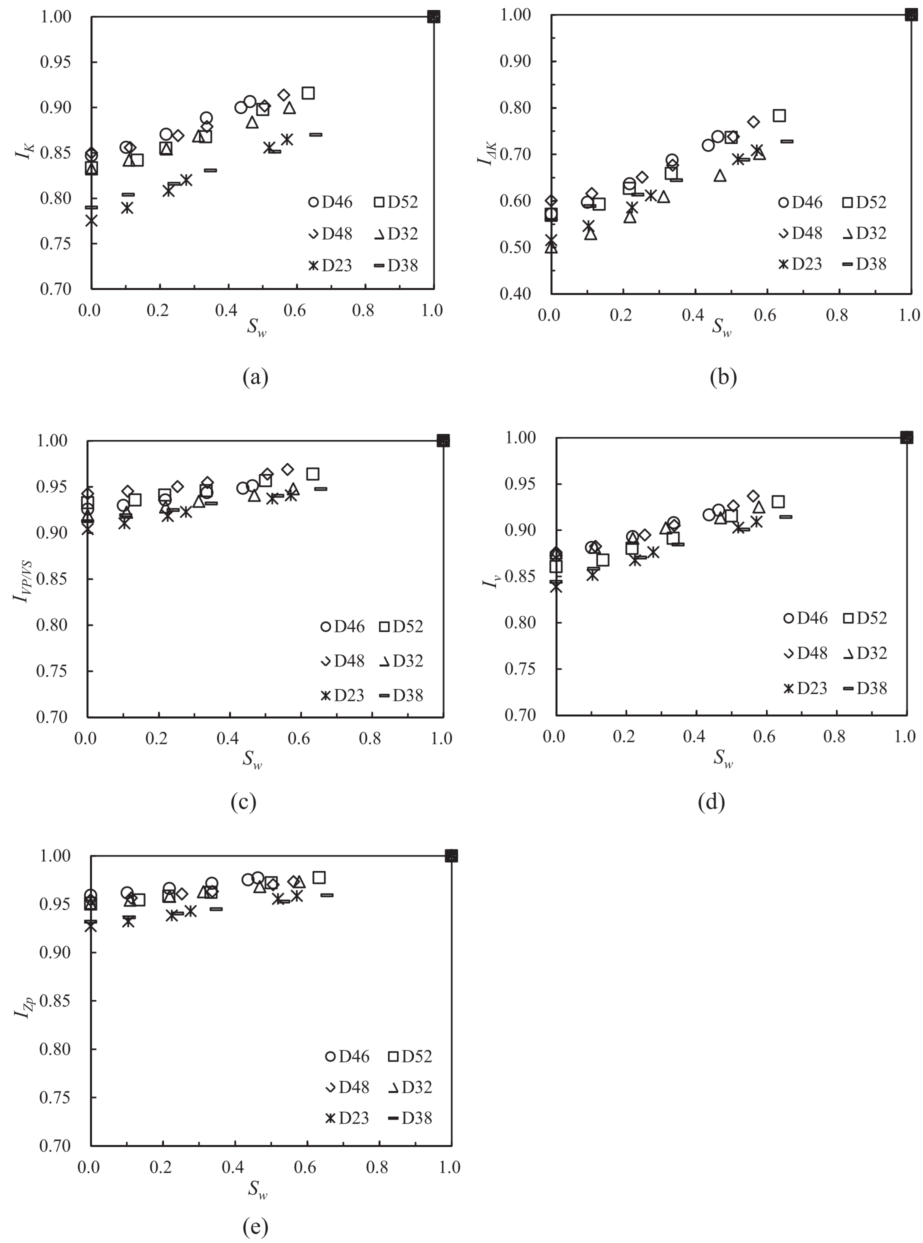

Fig. 1. Variation of various fluid factor indices with the water saturation for the water-oil saturated samples with different porosities from Daqing Oilfield, China. The distributions of the sample porosities are shown in Table 1.

under different porosities are shown in Fig. 2. Again, it can be found that these fluid factor indices all increase with the water saturation due to the increase of the sample bulk modulus with the water saturation. Comparing the sensitivities of these fluid factor indices to the water saturation, the following relation can be obtained: $I_{\Delta K} > I_K > I_\nu > I_{Zp} > I_{VP/Vs}$, which is similar to the case saturated with water-oil. With respect to the dependency on the porosity, we can obtain their relative degree of dependency by comparing the relative change of the fluid factor indices between the sample with largest and smallest porosity. The result is as follows: $I_{\Delta K} < I_K \approx I_{VP/VS} \approx I_{Zp} < I_\nu$. Hence, for the fluid saturation estimation in the water-gas saturated sandstone, $I_{\Delta K}$ is still the best fluid factor index and I_K and I_ν are secondary which are better than I_{Zp} and $I_{VP/Vs}$. This is similar with the case saturated with water-oil mixture.

4. Theoretical simulation

4.1. Methodology

To validate the experimental results, we carry out the theoretical simulations on the variations of the fluid factor indices with the water saturation under different porosities. In the calculation of the fluid factor indices, the elastic properties of the samples are required as shown in equations (4), (7) and (11)–(13). For the samples with multiphase saturation, the distribution of the fluid pressure within the samples has significant influences on their elastic properties (Johnson, 2001). Hence, different methodologies are applied to calculate the elastic properties of the samples with different fluid pressure distribution at the ultrasonic frequencies.

For the water-oil saturated samples, due to the similar elastic properties between water and oil, the fluid pressure within the

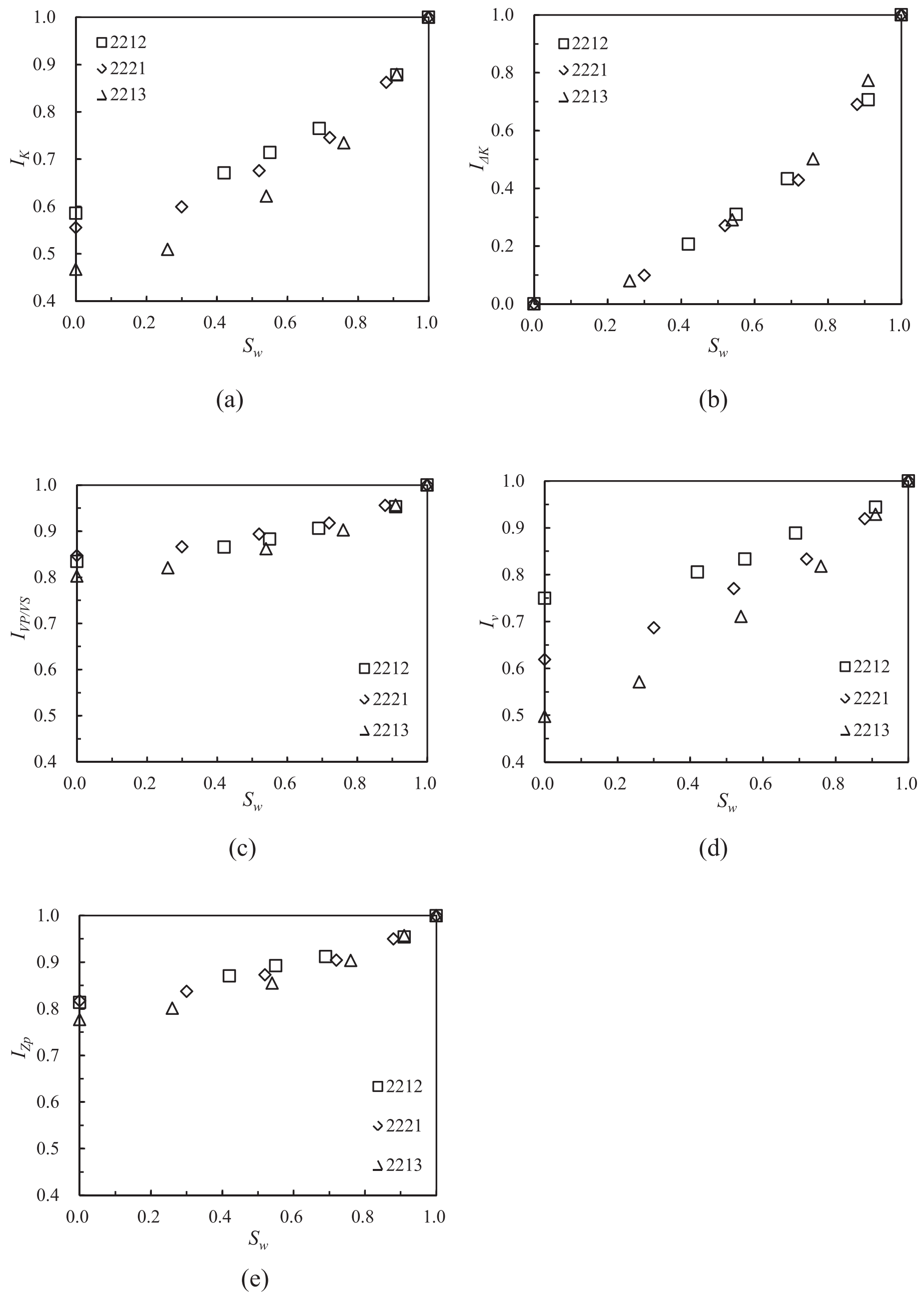

Fig. 2. Variation of various fluid factor indices with the water saturation for the water-gas saturated samples with different porosities from Xinjiang Oilfield, China. The distributions of the sample porosities are shown in Table 2.

water phase and the oil phase is close to each other. Therefore, the fluid pressure normally can equilibrate throughout the sample in a short time. This means that the fluid pressure in the water-oil saturated samples should be uniform at the ultrasonic frequencies. Under this condition, we can apply the Gassmann – Wood equation to calculate their elastic properties (e.g., Gregory, 1976; Murphy, 1984; Mavko and Mukerji, 1998; Johnson, 2001). The Wood equation (Wood, 1955) is applied first to obtain the effective elastic property of the water-oil mixture as follows:

$$K_f = \frac{1}{\frac{1-S_w}{K_{oil}} + \frac{S_w}{K_w}}, \tag{14}$$

where K_f is the effective bulk modulus of the water-oil mixture; K_{oil} and K_w are the bulk modulus of the oil and water, respectively; S_w is the water saturation.

Then, the elastic properties of the water-oil saturated samples can be obtained using the Gassmann equation as follows:

$$K_{wo} = K_{dry} + \frac{\left(1 - K_{dry}/K_s\right)^2}{\frac{\phi}{K_f} + \frac{1-\phi}{K_s} - \frac{K_{dry}}{K_s^2}}, \tag{15}$$

$$G_{wo} = G_{dry}, \tag{16}$$

where K_{wo} and G_{wo} are the bulk and shear moduli of the sandstone saturated with water-oil mixture; K_s is the bulk modulus of the sand grains; K_{dry} and G_{dry} are the bulk and shear moduli of the dry sandstone, respectively; Φ is the sample porosity. The fluid factor indices can thus be calculated using equations (4), (7) and (11)–(13).

For the water-gas saturated samples, due to the great difference between the elastic properties of the water and the gas, the fluid pressure within the water phase and the gas phase will be significantly different. Hence, it is usually difficult for the fluid pressure to equilibrate within the water-gas mixture in a short time. This means the fluid pressure of the region of the samples saturated with water is usually different from that saturated with gas at the ultrasonic frequencies. In this case, the elastic properties of the samples can be computed using the Gassmann-Hill equation (e.g., Cadoret et al., 1995; Johnson, 2001; Lebedev et al., 2009; Caspari et al., 2014). The Gassmann equation is first applied to calculate the elastic properties of the region saturated with water and that saturated with gas, respectively. The corresponding equations are shown in equations (15) and (16) with K_f replaced by water bulk modulus K_w and gas bulk modulus K_g, respectively. Then, Hill equation (Hill, 1963, 1964) is used to calculate the elastic properties of the sample with water-gas saturation as follows:

$$K_{wg} = \frac{1}{\frac{S_w}{K_1+4/3G_{dry}} + \frac{1-S_w}{K_2+4/3G_{dry}}} - 4/3G_{dry}, \tag{17}$$

$$G_{wg} = G_{dry}, \tag{18}$$

where K_{wg} and G_{wg} are the bulk and shear moduli of the samples with water-gas saturation; K_1 and K_2 are the bulk modulus of the region saturated with water and that saturated with gas, respectively.

The above equations show that, to calculate the elastic properties of the saturated samples, the dry sample elastic properties are needed. Since the samples investigated in this paper are consolidated sandstones with medium values of porosities, we can use the self-consistent theory to obtain the dry sample elastic properties (Berryman, 1980, 1995). The equations for the self-consistent theory are as follows:

$$(1-\phi)\left(K_s - K_{dry}\right)P_1 - \phi K_{dry}P_2 = 0, \tag{19}$$

$$(1-\phi)\left(G_s - G_{dry}\right)Q_1 - \phi G_{dry}Q_2 = 0, \tag{20}$$

where Φ is the porosity of the sandstone; K_s and G_s are the bulk and shear moduli of the sand grains, respectively. The values of P_1 and Q_1 depend on the shape of the sand grains and those of P_2 and Q_2 depend on the shape of the pores. Here, we assume that the sand grains are spheres (aspect ratio $\alpha_1 = 1$), which have the following expressions for P_1 and Q_1 (Mavko et al., 2009):

$$P_1 = \frac{K_{dry} + 4/3G_{dry}}{K_s + 4/3G_{dry}}, \tag{21}$$

$$Q_1 = \frac{6\left(K_{dry}+2G_{dry}\right)G_{dry} + G_{dry}\left(9K_{dry}+8G_{dry}\right)}{6\left(K_{dry}+2G_{dry}\right)G_s + G_{dry}\left(9K_{dry}+8G_{dry}\right)}, \tag{22}$$

where K_s and G_s are the bulk and shear moduli of the sand grains, respectively.

The pores are assumed to be oblate spheroids which have the aspect ratio α_2. The corresponding expressions for P_2 and Q_2 are as follows (Mavko et al., 2009):

$$P_2 = \frac{K_{dry}\left(3K_{dry}+4G_{dry}\right)}{\pi\alpha_2 G_{dry}\left(3K_{dry}+G_{dry}\right)}, \tag{23}$$

$$Q_2 = \frac{1}{5}\left[1 + \frac{8G_{dry}\left(3K_{dry}+4G_{dry}\right)}{\pi\alpha_2 G_{dry}\left(3K_{dry}+4G_{dry}\right) + 2\pi\alpha_2 G_{dry}\left(3K_{dry}+G_{dry}\right)} + \frac{4/3\left(3K_{dry}+4G_{dry}\right)}{\pi\alpha_2\left(3K_{dry}+G_{dry}\right)}\right]. \tag{24}$$

By applying the iteration algorithm based on equations (19) and (20), the dry elastic properties of the samples can be obtained. Then the elastic properties of the water-oil and water-gas saturated samples can be calculated. The fluid factor indices are thus computed using their definitions.

4.2. Parameters

To compare the theoretical simulation results with the experimental results, we use the properties of the sandstone samples used in the experiments for the theoretical simulations. These sandstone samples are primarily composed of quartz sands and have little clay content. Hence, we take the bulk and shear moduli of the sand grains as 37 GPa and 44 GPa, respectively (Mavko et al., 2009). The porosities of these samples are distributed from 0.1 to 0.2 with an interval of 0.05. The aspect ratio of the pores is set to be 0.1 (Xu and White, 1995). The bulk moduli and the densities of the water, oil, and gas are given based on the in-situ confining pressure (23 MPa) and temperature (40 °C) of the formations, as shown in Table 3.

5. Results and comparison

The variations of the various fluid factor indices with the water saturation for the water-oil saturated samples with different porosities are shown in Fig. 3. It can be seen that $I_{\Delta K}$ is most sensitive to the water saturation and its sensitivity to the water saturation is almost independent of the porosity. This can be explained using Gassmann equation. Substituting the Gassmann equation into equations (5) and (6) yields:

$$\Delta K = \frac{\left(1 - K_{dry}/K_s\right)^2}{\frac{\phi}{K_f} + \frac{1-\phi}{K_s} - \frac{K_{dry}}{K_s^2}}, \tag{25}$$

$$\Delta K_0 = \frac{\left(1 - K_{dry}/K_s\right)^2}{\frac{\phi}{K_w} + \frac{1-\phi}{K_s} - \frac{K_{dry}}{K_s^2}}. \tag{26}$$

Since K_s is usually much larger than K_f and K_w, equations (25) and (26) can be approximated as:

Table 3
Properties of saturating fluids.

Water		Oil		Gas	
Modulus (GPa)	Density (g/cc)	Modulus (GPa)	Density (g/cc)	Modulus (GPa)	Density (g/cc)
2.627	1.029	0.903	0.7	0.01	0.065

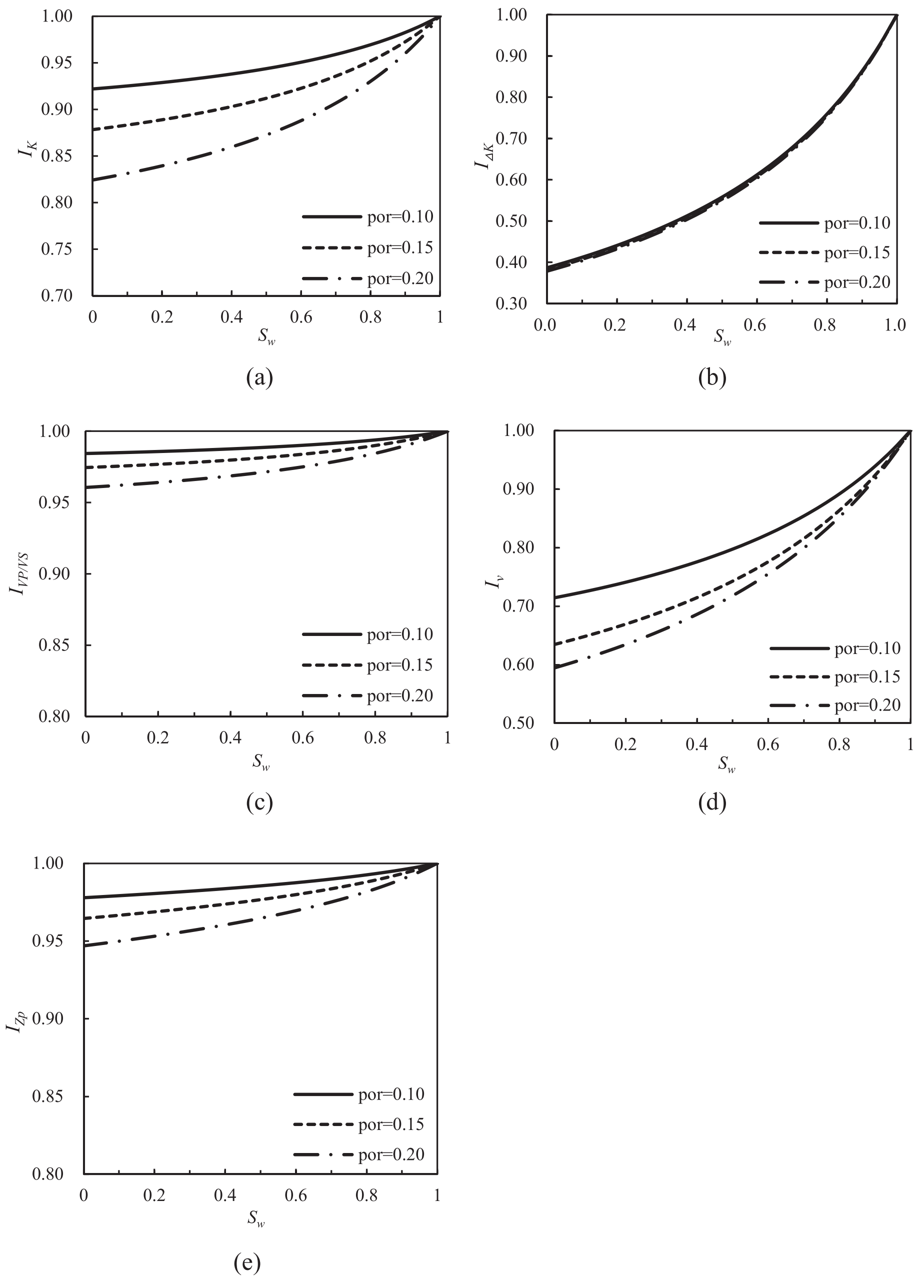

Fig. 3. Theoretical simulations of the variations of the various fluid factor indices with the water saturation for the water-oil saturated samples with different porosities.

$$\Delta K \approx \frac{\left(1 - K_{dry}/K_s\right)^2 K_f}{\phi}, \tag{27}$$

$$\Delta K_0 \approx \frac{\left(1 - K_{dry}/K_s\right)^2 K_w}{\phi}. \tag{28}$$

Hence, substituting equations (27) and (28) into equation (7) and using equation (14) yield:

$$I_{\Delta K} \approx (1 - S_w)\frac{K_{oil}}{K_w} + S_w. \tag{29}$$

Equation (29) shows that $I_{\Delta K}$ is independent of the rock porosities, which explains the observations from the theoretical simulations and the experimental results. We can also see that the sensitivity of $I_{\Delta K}$ to water saturation depends on the ratio of K_{oil} to K_w. In our case, K_w is almost three times larger than K_{oil}, hence, $I_{\Delta K}$ has high sensitivity to the water saturation. In fact, the sensitivities of the other fluid factor indices to the water saturation are also related to the ratio of K_{oil} to K_w. Once K_{oil} is equal to K_w, all the fluid factor indices will have no sensitivity to the water saturation as the oil and water will have the same effects on the elastic properties of the rocks. Hence, the sensitivities of all the fluid factor indices to the water saturation will change simultaneously with the ratio of K_{oil} to K_w. This implies that $I_{\Delta K}$ may be always more sensitive to the water saturation than the other fluid factor indices for any ratio of K_{oil} to K_w. It can also be found that I_K and I_ν are more sensitive to the water saturation and less dependent on the porosity than $I_{VP/VS}$ and I_{Zp}. All these observations from theoretical simulations are qualitatively consistent with the experimental results.

The variations of the fluid factors with the water saturation for the water-gas saturated samples with different porosities are shown in Fig. 4. Again, it is found that $I_{\Delta K}$ is most sensitive to the water saturation and its variation with the water saturation is almost independent of the rock porosities. Similar with the case saturated with water-oil mixture, we can obtain the following approximation for $I_{\Delta K}$ for the samples saturated with water-gas mixture:

$$I_{\Delta K} \approx \frac{AS_w}{1 - S_w + A}, \tag{30}$$

where

$$A = \frac{K_{dry} + 4\big/3G_{dry}}{\Delta K_0}, \tag{31}$$

ΔK_0 is the bulk modulus increment due to the saturation of the water, as shown in equation (6).

As the bulk modulus increment ΔK_0 is usually much smaller than the dry sample compressional wave modulus (K_{dry}+4/3G_{dry}), the value of A should be much larger than 1. Hence, we can obtain that $I_{\Delta K} \approx S_w$. This means that $I_{\Delta K}$ is almost proportional to the water saturation and has the highest sensitivity to the water saturation compared to the other fluid factor indices (as the relative change of the other fluid factor indices from $S_w = 0$ to $S_w = 1$ can't exceed 1). It also shows that the rock porosities have little effects on the value of $I_{\Delta K}$. These explain the observations from the theoretical

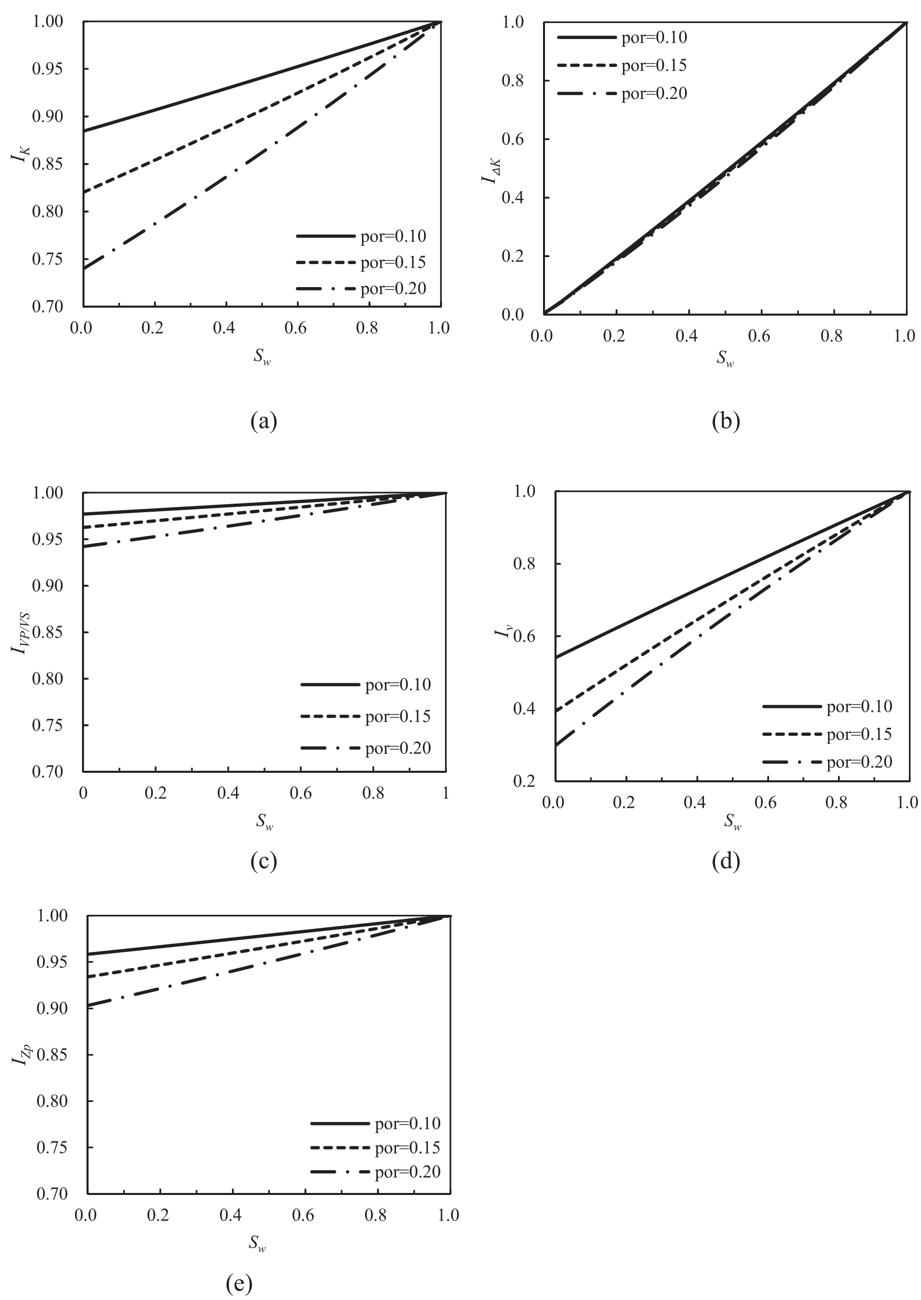

Fig. 4. Theoretical simulations of the variations of the various fluid factor indices with the water saturation for the water-gas saturated samples with different porosities.

simulations and experimental results. Besides $I_{\Delta K}$, it can also be observed that I_K and I_ν are better than $I_{VP/VS}$ and I_{Zp} considering both their sensitivities to the water saturation and the dependencies on the porosities. These observations agree with the experimental results qualitatively.

In summary, from both the theoretical simulations and the experimental results, we can draw the same conclusions for the fluid factor indices in both the water-oil and water-gas saturated sandstone reservoirs: 1) $I_{\Delta K}$ is most sensitive to the water saturation and its variation with the water saturation is almost independent of the rock porosities. Hence, it is an ideal fluid factor index for the fluid saturation estimation. 2) Apart from $I_{\Delta K}$, I_K and I_ν are also good fluid factor indices, which are more sensitive to the water saturation and less dependent on the rock porosities than $I_{VP/VS}$ and I_{Zp}.

6. Discussion

6.1. Discrepancy between theoretical simulation and experimental results

While the theoretical simulations agree with the experimental results qualitatively on the whole, some discrepancies exist between them, especially for I_ν. There are two possible reasons for the discrepancies. One is that the fluid pressure in the samples with water-oil or water-gas saturation doesn't satisfy the assumptions of the Gassmann-Wood or Gassmann-Hill equation. This means the fluid pressure in the samples have some time to diffuse, but not enough time to reach the status of uniform pressure distribution. Hence, the fluid pressure in the samples will be neither uniform nor isolated within each fluid phase. As a result, the samples will have the elastic properties that are between the upper bound given by Gassmann-Hill equation and the lower bound given by Gassmann-Wood equation (Lebedev et al., 2009). The theoretical simulations based on Gassmann-Wood and Gassmann-Hill bounds will thus deviate from the experimental results. The other possible reason is that the dry sample elastic properties calculated by the self-consistent theory may not be accurate. This may be caused by the inaccurate sand grain moduli and pore aspect ratio used by theoretical simulations. Furthermore, the self-consistent theory itself is not an exact solution for the rock elastic properties. Instead, it is an approximation for the elastic properties of the rocks with medium values of porosities. This also brings some errors to the theoretical simulation results.

6.2. Effects of confining pressure and temperature

As the change of the sample elastic properties or the fluid factor indices with the varying confining pressure and temperature are not measured or simulated, the exact influences of confining pressure and temperature are unknown. However, these influences should be small in our case according to the previous studies. The influences of the confining pressure on the rock elastic properties can be significant if the rocks contain some fractures (e.g., Kuster and Toksöz, 1974; Mavko et al., 1995; Glubokovskikh et al., 2016). The confining pressure will close the fractures, especially the micro-cracks, in the rocks, which causes the increase of the rock stiffness. Nevertheless, few fractures are observed in the samples investigated in this paper. Hence, the confining pressure should have small influences on the sample elastic properties, and therefore, the fluid factor indices. For the temperature, its influences on the elastic properties and fluid factor indices of these samples should also be small. The temperature primarily have effects on the elastic properties of the saturating fluids. For the fluids with high viscosity, such as the heavy oil, the temperature will greatly influence their elastic properties, and hence the elastic properties of the samples saturated with these fluids (Han et al., 2007; Guo and Han, 2016). Since the samples in this paper are saturated with the fluids that have low viscosity, the temperature has little effects on the elastic properties of the fluids. Hence, the elastic properties and the fluid factor indices of the samples should be little affected by the temperature.

6.3. Application of fluid factor indices on fluid saturation estimation

This study proposes the fluid factor indices and investigates their fluid saturation sensitivity and porosity dependency, which provides the basis for using them in the fluid saturation estimation in the future. To apply them on the fluid saturation estimation, we need to establish the quantitative relations between the fluid factor indices and the fluid saturation. These relations can be established through the theoretical derivations, as shown in equations (29) and (30) for $I_{\Delta K}$. They can also be obtained by correlating the fluid factor indices with the fluid saturation through the experimental data. This is one topic we will study in detail in the future.

After obtaining these quantitative relations, the fluid saturation can be estimated from the sonic logging or seismic data. The fluid factor indices can first be calculated from the acoustic velocity and density data provided by the sonic logging or seismic data. Then the fluid saturation can be obtained from the fluid factor indices through the established relations. Here, it should be noted that, in the calculation of the fluid factor indices, we need to know the value of the fluid factor under the full water saturation. This can be obtained from the adjacent formations which are saturated with water and have similar porosities. However, it is not always convenient to obtain this value. Hence, to enable the more convenient estimation of the fluid saturation, we can define the acoustic formation factor and establish their relations with the porosity. Combing the acoustic formation factor and the fluid factor index will enable us to calculate the fluid saturation from the sonic logging or seismic data in a similar way with using the resistivity or conductivity logging data to estimate the fluid saturation from the Archie's formula. This is another topic that we will investigate in the future.

Another thing that should be noted is that when using the sonic logging or seismic data to calculate the fluid factor indices, the quality of the sonic logging or seismic data may be influenced by the borehole environment and other factors. Hence, they may need to be corrected before using them to calculate the fluid factor indices. To correct the data, we first need to find the primary influencing factors to the data quality, then we can use the corresponding correction methods. The study of the correction methods is beyond the scope of this paper.

7. Conclusions

In this work, we propose the fluid factor indices for the fluid saturation estimation. The fluid factor index is defined as the ratio of the value of the fluid factor for rocks with oil/gas-water saturation to the corresponding value under the full water saturation, which is similar to the resistivity index in the Archie's formula. This definition of fluid factor index can largely cancel out the influences of rock porosities and hence primarily reflects the effects of fluid saturation. We then study five fluid factor indices (I_K, $I_{\Delta K}$, $I_{VP/VS}$, I_ν, and I_{Zp}), which are calculated from sample bulk modulus, bulk modulus increment due to fluid saturation, compressional to shear velocity ratio, Poisson's ratio, and compressional wave impedance, respectively. The sensitivity of these fluid factor indices to the fluid saturation and their dependency on the rock porosities are investigated through the ultrasonic experiments on the water-oil and water-gas saturated sandstone samples. The results show that, for both the water-oil and water-gas saturated samples, $I_{\Delta K}$ is an ideal fluid factor index for fluid saturation estimation as it is most sensitive to the fluid saturation and is almost independent of the rock porosities; I_K and I_ν are not as good as $I_{\Delta K}$, but are better than $I_{VP/VS}$ and I_{Zp} with respect to their sensitivity to the fluid saturation and dependency on the rock porosities. Hence, $I_{\Delta K}$ is recommended to be used for the fluid saturation estimation. These experimental observations are further validated and explained by the theoretical simulations.

In the discussion part, the possible reasons for the discrepancies between the experimental results and the theoretical simulations are analyzed. Furthermore, the potential influences of confining pressure and temperature on the results are discussed. Finally, the steps of applying the fluid factor indices on the fluid saturation estimation and the problems that may be encountered in this procedure are discussed. This research provides the basis for the fluid saturation estimation using the acoustic (sonic logging or seismic) data, which is very helpful to the oil/gas exploration and production.

Acknowledgement

We would like to thank the financial support from National Natural Science Foundation of China, Contract U1562108, and the data provided by Daqing and Xinjiang Oil Field of China.

References

Ara, T.S., Talabani, S., Vaziri, H.H., Islam, M.R., 2001. In Depth Investigation of the Validity of the Archie Equation in Carbonate Rocks. SPE Production and Operation Symposium, 67204, Oklahoma City, Oklahoma, USA.
Archie, G.E., 1942. The electrical resistivity log as an aid in determining some reservoir characteristics. Pet. Trans. AIME 146, 54–62.
Batzle, M., Hofmann, R., Han, D.–H., Castagna, J., 2001. Fluid and frequency dependent seismic velocity of rocks. Lead. Edge 20 (no. 2), 168–171.
Berryman, J.G., 1980. Long-wavelength propagation in composite elastic media. J. Acoust. Soc. Am. 68, 1809–1831.
Berryman, J.G., 1995. Mixture theories for rock properties. In: Ahrens, T.J. (Ed.), Rock Physics and Phase Relations: a Handbook of Physical Constants. American Geophysical Union, pp. 205–228.
Cadoret, T., Marion, D., Zinszner, B., 1995. Influence of frequency and fluid distribution on elastic wave velocities in partially saturated limestones. J. Geophys. Res. 100, 9789–9803.
Caspari, E., Qi, Q., Lopes, S., Lebedev, M., Gurevich, B., Rubino, J.G., Velis, D.R., B.Clennell, M., Müller, T.M., 2014. Wave attenuation in partially saturated porous rocks: new observations and interpretations across the scales. Lead. Edge 33 (no. 6), 606–614.
Clavier, C., Coates, G., Dumanoir, J., 1984. Theoretical and experimental bases for the dual water model for the interpretation of shaly sands. SPE J. 4, 153–168.
Gao, J., Wang, D., Liu, J., Sui, H., 2015. Theory study on fractured-vuggy reservoirs resistivity based on dual and triple porosity models. Well Logging Technol. 39 (no. 3), 277–282.
Gassmann, F., 1951. Über die Elastizität poroser medien: Veirteljahrsschrift der Naturforschenden Gesellschaft in Zürich, vol. 96, pp. 1–23.
Glubokovskikh, S., Gurevich, B., Lebedev, M., Mikhaltsevitch, V., Tan, S., 2016. Effect of asperities on stress dependency of elastic properties of cracked rocks. Int. J. Eng. Sci. 98, 116–125.
Gregory, A.R., 1976. Fluid saturation effects on dynamic elastic properties of sedimentary rocks. Geophysics 41 (no.5), 895–921.
Guo, J., Han, X., 2016. Rock physics modelling of acoustic velocities for heavy oil sand. J. Pet. Sci. Eng. 145, 436–443.
Hamada, G.M., Almajed, A.A., Okasha, T.M., Algathe, A.A., 2013. Uncertainty analysis of Archie's parameters determination techniques in carbonate reservoirs. J. Pet. Explor. Prod. Technol. 3 (no. 1), 1–10.
Han, D.-H., Batzle, M.L., 2004. Gessmann's equation and fluid saturation effects on seismic velocities. Geophysics 69 (no. 2), 398–405.
Han, D.-H., Yao, Q., Zhao, H.-Z., 2007. Complex Properties of Heavy Oil Sand, 77th Annual International Meeting, SEG, Expanded Abstracts, pp. 1609–1613.
Hill, R., 1963. Elastic properties of reinforced solids: some theoretical principles. J. Mech. Phys. Solids 11, 357–372.
Hill, R., 1964. Theory of mechanical properties of fibre-strengthened materials: I. Elastic behavior. J. Mech. Phys. Solids 12, 199–212.
Hilterman, F.J., 1989. Is AVO the Seismic Signature of Rock Properties, 59th SEG annual meeting, p559, Dallas, USA.
Johnson, D.L., 2001. Theory of frequency dependent acoustic in patchy-saturated porous media. J. Acoust. Soc. Am. 110 (no. 2), 682–694.
Kuster, G.T., Toksöz, M.N., 1974. Velocity and attenuation of seismic waves in two-phase media: part I: theoretical formulations. Geophysics 39 (no. 5), 587–606.
Lebedev, M., Toms-Stewart, J., Clennell, B., Pervukhina, M., Shulakova, V., Paterson, L., Müller, T., Gurevich, B., Wenzlau, F., 2009. Direct laboratory observation of patchy saturation and its effects on ultrasonic velocities. Lead. Edge 28 (no. 1), 24–28.
Mavko, G., Mukerji, T., 1998. Bounds on low-frequency seismic velocities in partially saturated rocks. Geophysics 63, 918–924.
Mavko, G., Mukerji, T., Dvorkin, J., 2009. The Rock Physics Handbook: Tools for Seismic Analysis in Porous Media. Cambridge University Press.
Mavko, G., Mukerji, T., Godfrey, N., 1995. Predicting stress-induced velocity anisotropy in rocks. Geophysics 60 (no. 4), 1081–1087.
Murphy, W.F., 1984. Acoustic measures of partial gas saturation in tight sandstones. J. Geophys. Res. 89, 11549–11559.
Ning, Z., He, Z., Huang, D., 2006. High sensitive fluid identification based on seismic data. Geophys. Prospect. Pet. 45 (no.3), 239–241.
Olsen, C., Hongdul, T., Lykke Fabricius, I., 2008. Prediction of Archie's cementation factor from porosity and permeability through specific surface. Geophysics 73, E81–E87.
Rezaee, M.R., Motiei, H., Kazemzadeh, E., 2007. A new method to acquire m exponent and tortuosity factor for microscopically heterogeneous carbonates. J. Pet. Sci. Eng. 56, 241–251.
Russell, B.H., Hedlin, K., Hilterman, F.J., Lines, L.R., 2003. Fluid-property discrimination with AVO: a Biot – Gassmann perspective. Geophysics 68 (no. 1), 29–39.
Salem, H.S., Chilingarian, G.V., 1999. The cementation factor of Archie's equation for shaly sandstone reservoirs. J. Pet. Sci. Eng. 23 (no.2), 83–93.
Teh, W.J., WIllhite, G.P., Doveton, J.H., Tsau, J.S., 2011. Improved Predictions of Porosity from Microresistivity Logs in a Mature Field through Incorporation of Pore Typing. SPE Eastern Regional Meeting, 149506, Columbus, Ohio, USA.
Waxman, M.H., Smits, L.J.M., 1968. Electrical conductivities in oil-bearing shaly sands. SPE J. 8, 107–122.
Wood, A.W., 1955. A Text Book of Sound. McMillan Co.
Xu, S., White, R.E., 1995. A new velocity model for clay-sand mixture. Geophys. Prospect. 43, 91–118.
Yin, X., Zong, Z., Wu, G., 2015. Research on seismic fluid identification driven by rock physics. Sci. China Earth Sci. 58 (no. 2), 159–171.